Published in final edited form as:
J Immunol. 2011 April 15; 186(8): 4994–5003. doi:10.4049/jimmunol.1003010.

A UNIQUE HYBRID RENAL MONONUCLEAR PHAGOCYTE ACTIVATION PHENOTYPE IN MURINE SLE NEPHRITIS

Ramalingam Bethunaickan[*], **Celine C. Berthier**[†], **Meera Ramanujam**[*], **Ranjit Sahu**[*], **Weijia Zhang**[‡], **Yezou Sun**[‡], **Erwin Bottinger**[‡], **Lionel Ivashkiv**[§], **Matthias Kretzler**[†], and **Anne Davidson**[*,¶]

[*]Center for Autoimmunity and Musculoskeletal Diseases, Feinstein Institute for Medical Research, Manhasset, New York, NY 11030

[†]Department of Medicine, University of Michigan Medical School, Ann Arbor, MI 48109

[‡]Department of Medicine, Mount Sinai Medical Center, New York, NY 10029

[§]Weill Cornell Graduate School of Medical Sciences, New York, NY 10021

Abstract

Renal infiltration with mononuclear cells is associated with poor prognosis in SLE. A renal macrophage/dendritic cell signature is associated with onset of nephritis in NZB/W mice and immune modulating therapies can reverse this signature and the associated renal damage despite ongoing immune complex deposition. In nephritic NZB/W mice renal F4/80^{hi}/CD11c^{int} macrophages are located throughout the interstitium whereas F4/80^{lo}/CD11c^{hi} dendritic cells accumulate in perivascular lymphoid aggregates. We show here that F4/80^{hi}/CD11c^{int} renal macrophages have a Gr1^{lo}/Ly6C^{lo}/VLA4^{lo}/MHCII^{hi}/CD43^{lo}/CD62L^{lo} phenotype, different to that described for inflammatory macrophages. At nephritis onset F4/80^{hi}/CD11c^{int} cells upregulate cell surface CD11b, acquire cathepsin and MMP activity and accumulate large numbers of autophagocytic vacuoles; these changes reverse after induction of remission. Latex bead labeling of peripheral blood Gr1^{lo} monocytes indicates that these are the source of F4/80^{hi}/CD11c^{int} macrophages. CD11c^{hi}/MHCII^{lo} dendritic cells are found in the kidneys only after proteinuria onset, turnover rapidly, and disappear rapidly after remission induction. Gene expression profiling of the F4/80^{hi}/CD11c^{int} population displays increased expression of pro-inflammatory, regulatory and tissue repair/degradation associated genes at nephritis onset that reverses with remission induction. Our findings suggest that mononuclear phagocytes with an aberrant activation profile contribute to tissue damage in lupus nephritis by mediating both local inflammation and excessive tissue remodeling.

INTRODUCTION

Renal mononuclear phagocyte infiltration in human SLE nephritis is associated with poor disease outcome (1) and is intricately linked with activation of the endothelium, renal chemokine production, proteinuria, complement activation, progressive hypoxia and hypertension (2, 3). In NZB/W SLE-prone mice both Fc receptor mediated interaction of mononuclear cells with renal immune complexes and mononuclear cell renal infiltration are required for renal damage to occur (4).

Address Correspondence to: Anne Davidson, Feinstein Institute for Medical Research, 350 Community Drive, Manhasset NY 11030, Tel: 516 562 3840, Fax: 516 562 2953, adavidson1@nshs.edu.

[¶]This work was supported by the Alliance for Lupus Research (AD, EB, WZ), NIH grants R01 AI059636-01A2 (AD and LI) and NIH R01 DK085241-01 (CB, MK, EB, WZ, AD), the NY SLE Foundation and Rheuminations (RB).

Macrophages have distinct activation patterns and functions depending on the stimuli to which they are exposed (5–8). Classically activated (M1) macrophages, induced by TNFα/IFNγ or by IFNβ, have enhanced antigen presentation capabilities and secrete reactive oxygen intermediates, nitric oxide, chemokines and cytokines that induce a Th1 response. Alternatively activated (M2) macrophages, activated by IL-4 and IL-13 or induced in responses to helminthes, secrete protective cytokines such as IL-10 and IL1-RA. These cells express the mannose receptor, Arginase1 and the transcription factors YM1 and FIZZ-1 and are also capable of tissue repair (9). Other macrophage activation patterns represent a mixed phenotype likely resulting from simultaneous exposure to inflammatory and homeostatic/suppressive factors in vivo. Of relevance to SLE, macrophages exposed to immune complexes and TLR agonists are characterized by an IL-10^{hi}/IL-12^{lo} phenotype termed M2b (10). These cells have antigen presentation capabilities and may continue to produce inflammatory cytokines but they are not involved in tissue repair. A somewhat different phenotype is induced by ITAM crosslinking in vitro (11). These cells do not produce inflammatory cytokines but markedly upregulate IL-10 and CXCL13, a chemokine that facilitates lymphoid neogenesis.

Normal mouse kidneys have a heterogeneous population of mononuclear phagocytes. The dominant F4/80^{hi}/CX3CR1^{hi}/MHCII^{hi}/CD11b^{int}/CD11c^{int} renal macrophage population forms a network throughout the renal interstitium (12, 13). Normal human kidneys have a similar interstitial network of CD68 positive cells (14). In mice these intrinsic renal cells use dendrites to sample their local environment and they can present antigen, but they are poor NO producers and are only weakly phagocytic. This has suggested that they are more like dendritic cells (12, 13, 15, 16) and their nomenclature is now a subject of some debate (15). A minor population of mononuclear cells in normal kidneys is CD11b^{hi}/CD62L^{hi}/Ly6C^{hi}/Gr1^{int}/CCR2^{hi}/F4/80^{lo}/CD11c^{lo}/MHCII^{lo}/CD86^{lo}; during acute renal inflammation or ischemia this macrophage population increases markedly and secretes pro-inflammatory cytokines (17). Small populations of CD11b^{hi}/CD11c^{hi} and CD11b^{lo}/CD11c^{hi} renal dendritic cells have been described (18) but have not been well characterized.

In this study we analyzed the characteristics and function of the major renal mononuclear phagocyte populations from young and nephritic NZB/W mice and from mice in which remission of nephritis was induced with combination cyclophosphamide and costimulatory blockade (19). We show that CD11b^{+}/CD11c^{int}/F4/80^{hi} (F4/80^{hi}) cells, that are the dominant mononuclear cells in normal renal interstitium, acquire an activated phenotype during active nephritis that reverses upon remission induction. During active SLE nephritis F4/80^{hi} cells are a major renal source of several pro-inflammatory cytokines and chemokines (20) but they also secrete molecules associated with tissue protection and repair, that in excess may contribute to tissue degradation. In contrast, CD11b^{+}/CD11c^{hi}/F4/80^{lo} (CD11c^{hi}) cells, that are rare in normal kidneys, appear in large numbers in lymphoid aggregates during nephritis (20) and disappear upon remission induction. These two major populations of infiltrating mononuclear cells are topographically and functionally distinct from each other and are phenotypically different from the pro-inflammatory Gr1^{hi} macrophages that infiltrate kidneys during acute inflammatory glomerulonephritis or renal ischemia (17). Our data call into question the use of acute inflammatory models of nephritis in the study of chronic SLE and point to a unique hybrid activation phenotype of mononuclear phagocytes in chronic SLE nephritis that is closely associated with proteinuria onset and tissue damage and whose reversal is associated with remission induction.

MATERIALS and METHODS

Mice

NZB/NZW F1 females were purchased from Jackson Laboratories (Bar Harbor ME). Urine was tested weekly for proteinuria by dipstick (Fisher Scientific, Pittsburgh, PA). Once fixed proteinuria appeared, a single dose of cyclophosphamide and 6 doses of CTLA4Ig and anti-CD154 were administered as previously described (19). Mice were sacrificed 3–4 weeks after entering complete remission (≤ 30mg/dl proteinuria on at least 2 occasions 7 days apart). Nephritic mice were sacrificed 2–6 weeks after proteinuria onset but before the development of terminal renal failure. Young NZB/W F1 mice were sacrificed at 8–16 weeks of age. Kidneys were also obtained from 129/SvJ mice in which anti-GBM disease was induced 14 days previously exactly as described (21).

Flow cytometry and cell sorting

Single cell suspensions were prepared from perfused kidneys and stained with antibodies to CD11c, CD11b, CD4, CD8, B220, PDCA, VLA4, MHCII, CD80, CD86, CD43, CD44, CD62L, Gr-1, Ly6C (BD Pharmingen) and F4/80 (Caltag-Invitrogen, Carlsbad CA), as previously described (20, 22). CD11b+/CD11c^{hi}, and CD11b+/CD11c^{int}/F4/80^{hi} cells were isolated using a BD FACSAria IIu cell sorter. A dump gate for CD49b, CD4, CD8, CD5, and B220 was used to exclude NK cells and lymphocytes and DAPI was used to exclude dead cells. Isolated cells were >90% pure. Cytospin preparations of isolated cells were stained with Wright Giemsa stain.

The proteolytic activity of cathepsins (B, L and S) and matrix metalloproteinases (MMPs -2, -3, -9, and -13) were measured in vivo using activatable fluorescent sensors Prosense-680 and MMPsense-680 (Visen Medical, Bedford, MA, USA – (23)). 5 nmol of probe in 100 μl of sterile PBS was injected i.v. 24hr before sacrifice and kidney cells were stained with antibodies to CD11b, CD11c and F4/80 as above. F4/80^{hi} cells from nephritic and young mice were sorted into Prosense^{hi} and Prosense^{lo} populations and subjected to real-time PCR for IL-10, IKKε, Mincle, MMP14 and TIMP1. Results were normalized to β-Actin.

Electron Microscopy studies

For transmission EM studies, sorted renal cell pellets were fixed with 2.5% glutaraldehyde, 2% paraformaldehyde in 0.1 M sodium cacodylate buffer, postfixed with 1% osmium tetroxide followed by 2% uranyl acetate, dehydrated with ethanol and embedded in LX112 resin (LADD Research Industries, Burlington VT). Ultrathin sections were cut on a Reichert Ultracut UCT, stained with uranyl acetate followed by lead citrate and viewed on a JEOL 1200EX transmission electron microscope at 80kv.

For scanning EM studies, sorted cell pellets were quickfixed in 1% Osmium Tetroxide, 0.1 M sodium Cacodylate, 0.2 M Sucrose, 5mM $MgCl_2$ pH.4 (SEM buffer) for ten seconds, followed by 2.5% glutaraldehyde in SEM buffer. Secondary fixation was performed with 1% Osmium Tetroxide, in SEM buffer for 30 minutes, and pellets were dehydrated with ethanol. Pellets were then subjected to critical point dry using liquid carbon dioxide in a Tousimis Samdri 795 Critical Point Drier (Rockville, MD) followed by sputter coat with gold-palladium in a Denton Vacuum Desk-2 Sputter Coater (Cherry Hill, NJ). Samples were examined in a JEOL JSM6400 Scanning Electron Microscope (Peabody, MA), using an accelerating voltage of 10 KV.

BrdU incorporation

Mice were loaded i.p. with 10mg of bromodeoxyuridine (BrdU, Sigma-Aldrich, St. Louis, MA) followed by feeding with water containing 1 mg/ml BrdU for up to 60 days. Groups of

four mice were sacrificed at intervals and kidney cells were analyzed by flow cytometry as above, with the addition of anti-BrdU (BD Pharmingen) according to manufacturers' instructions. Similar experiments were performed in mice fed with BrdU for 7 or 15 days after nephritis onset. To determine whether remission was associated with migration of cells out of the kidneys we began BrdU feeding 48 hrs after initiation of the remission induction regimen and sacrificed mice 21 and 40 days later. In alternate experiments we fed mice with BrdU for >60 days from the time of remission until relapse. BrdU was then stopped and the mice were sacrificed 21 days later.

Labeling of peripheral blood monocytes with fluorescent beads

100ul of a 1:10 dilution of yellow-green fluorescent 1.0 μm latex particles (Polysciences, Warrington, PA) was injected i.v. per mouse. Peripheral blood and organs were harvested 3 days later and subjected to flow cytometry and immunohistochemical analysis. In alternate experiments, isolated kidney cells were exposed in vitro to latex beads for 30 or 45 minutes and analyzed by flow cytometry.

RNA Amplification, Labeling and GeneChip Array Hybridization

We performed Affymetrix microarrays of cDNA obtained from sorted NZB/W F4/80^{hi} cells from 6 young kidneys, 7 nephritic kidneys and 4 kidneys harvested 3–4 weeks after induction of complete remission. RNA was synthesized from sorted cell populations using picopure RNA isolation kit (Arcturus Molecular Device Corporation, Sunnyvale, CA). The quality of total RNA was assessed using a NanoDrop ND-1000 Spectrophotometer (Thermo Scientific, Wilmington, DE) and verified on a NanoRNA chip (Agilent, Santa Clara, CA).

30 ng of total RNA was amplified and labeled with biotin (Ovation Biotin system, NuGEN Technologies, Inc., San Carlos, CA), fragmented and hybridized to Affymetrix Mouse Genome 430 Plus 2.0 GeneChip arrays (Santa Clara, CA). Arrays were washed, stained, and scanned by GeneChip Scanner 3000 7G according to the Affymetrix Expression Analysis technical Manual.

CEL files were processed using GenePattern analysis pipeline (www.genepattern.com). Normalization was performed using the Robust Multichip Average (RMA) method and version 10 of the Mouse Entrez-Gene custom CDF annotation from Brain Array (http://brainarray.mbni.med.umich.edu/Brainarray/default.asp). The resulting data were log2transformed. Of the 16539 mouse genes represented on the Affymetrix genechip, 14415 were expressed above the 27 poly-A Affymetrix control expression baseline and used for further analyses. Unpaired significance analysis of microarrays (SAM) was performed for each statistical comparison between the relevant groups (prenephritic vs. nephritic F4/80^{hi} cells, nephritic vs. remission F4/80^{hi} cells and prenephritic vs. remission F4/80^{hi} cells). Genes regulated between 2 groups with a q-value (false discovery rate) below 5% were considered significant and gene lists of interest were uploaded for literature based pathway analyses on Genomatix Bibliosphere Pathway Edition software (www.genomatix.de). The data discussed in this publication have been deposited in NCBIs Gene Expression Omnibus (GEO, http://www.ncbi.nlm.nih.gov/geo/) and are accessible through GEO Series accession number GSE27045.

Real-time PCR

Verification of selected differentially expressed genes was performed using Custom TaqMan® Expression Arrays (Applied Biosystems) as per manufacturers' instructions. Five internal controls identified by the microarray analysis were tested and data were normalized to the mean of the three most stable control genes (Gus-B, Oaz1 and β-Actin) and then to the mean of the young controls. To identify significantly differentially expressed genes between

groups, Significance Analysis of Microarray (SAM, version 2.1)(24) was carried out. Genes regulated between 2 groups with a q-value (false discovery rate) below 5% were considered significant.

RESULTS

Remission induction using CTX and costimulatory blockade

We have previously reported that disappearance of proteinuria after remission induction therapy is associated with decreased glomerular damage and interstitial inflammation scores by light microscopy and with markedly increased longevity (19, 20). Remission of nephritis in the group of mice studied here was characterized by a disappearance of proteinuria from ≥ 300mg/dl to ≤ 30mg/dl on repeated measurements over a 2–4 week period, whereas untreated mice remained proteinuric. BUN levels remained within the normal range in the treated mice (22.0 +/− 8.1 vs. 22.8 +/− 2.6 in young mice; p = NS) whereas they increased in controls (49.6 +/− 25.0; $p < 0.001$ vs. both young and remission mice). A decrease in interstitial lymphocytic infiltration of the kidneys evaluated by quantitation of renal cells expressing B220, CD5, CD4, CD8 or CD49b was also observed in the remission mice compared with controls (Figure S1 and Figure 1B).

NZB/W kidneys contain several distinct mononuclear phagocyte populations

Renal $CD11b^{+}$ and $CD11c^{+}$ mononuclear phagocytes in the kidneys of young, nephritic and remission mice were analyzed by flow cytometry using the gating strategy shown in Figure S1. The major ($F4/80^{hi}$) population in young mice had a phenotype similar to that of renal dendritic cells, namely $CD11b^{hi}/CD11c^{int}/F4/80^{hi}/Gr1^{lo}/Ly6C^{lo}/VLA4^{lo}/MHCII^{hi}/CD43^{lo}/CD62L^{lo}$ (17). A smaller population of cells ($F4/80^{lo}$) was $CD11b^{hi}/CD11c^{int}/F4/80^{lo}/Gr1^{lo}$. A third, infrequent population ($CD11c^{hi}$) was $CD11b^{hi}/CD11c^{hi}/F4/80^{lo}/Gr1^{lo}/MHC^{hi}/CD43^{hi}/CD62L^{lo}$ (Figure 1). A fourth population, comprising <2% of all cells in the lymphocyte/monocyte gate, was $CD11b^{lo}/CD11c^{hi}/F4/80^{lo}/Gr1^{lo}$ and may correspond to the $CD103^{+}$ population found in other tissues (25). Finally, <0.5% of all cells in the lymphocyte/monocyte gate had a pDC phenotype ($B220^{+}/PDCA^{hi}$). The latter two populations did not increase in frequency during the disease course and were not studied further. $CD11b^{hi}$ cells increased by 3–4 fold in nephritic kidneys compared with young kidneys (Figure 1A, B). The $F4/80^{hi}$ subset increased by 2–3 fold and upregulated surface expression of CD11b, F4/80, Ox40L and CD80 (20). These cells were also $MHC^{hi}/VLA4^{lo}/CD43^{lo}$ (Figure 1C, D) The $CD11c^{hi}$ subset underwent 10 fold expansion (Figure 1A, B) and was $MHCII^{lo}/VLA4^{hi}/CD43^{hi}$ (Figure 1C, D). The $F4/80^{lo}$ subset expanded 3 fold during nephritis but remained a minor population (Figure 1A, B). Few neutrophils ($CD11b^{hi}/F4/80^{-}/Gr1^{hi}$) were detected either before or during nephritis (Figure 1E). The renal $CD11b^{+}$ population of mice in complete remission resembled that of young prenephritic mice (Figure 1A, B). Importantly, we could not identify the $CD11b^{hi}/CD11c^{lo}/F4/80^{lo}/VLA4^{hi}/Ly6C^{hi}$ population reported by others in acute models of renal inflammation including anti-GBM disease (Figure S1 H–I). Conversely, the $CD11c^{hi}$ population we identified in nephritic NZB/W mice was not increased in frequency in mice with anti-GBM disease (data not shown).

Cell turnover rates of the major mononuclear phagocyte populations

Using BrdU incorporation we determined that the $CD11c^{hi}$ population had a renal half-life of 6.5 days in young mice. In contrast, the $F4/80^{hi}$ population had a half life of 16 days (Figure 2A); this did not increase in nephritic mice. To analyze the fate of $CD11b^{hi}$ cells during remission we administered BrdU starting 48 hours after initiation of remission induction. At Day 21, 64.6 +/− 8.7% of the $F4/80^{hi}$ population was still $BrdU^{-}$ (Figure 2C, D), indicating that the cells had not proliferated or been replaced by newly formed cells. In

contrast, splenic CD11b^{hi} cells were nearly all BrdU^{+} (Figure 2E). Even 40 days after remission induction 32.7 +/− 6.7% of the renal F4/80^{hi} population remained BrdU$^{−}$ (Figure 2F). Both BrdU^{+} and BrdU$^{−}$ populations in remission kidneys downregulated CD11b expression (MFI 41900 +/− 15338 in remission mice vs. 74860 +/− 16222 in nephritic controls; $p<0.04$ - compare Figure 2B with 2C and 2F). In contrast, at Day 21, all remaining CD11c^{hi} cells were BrdU^{+}, confirming the rapid turnover of this population (Figure 2D). In an alternate experiment we administered BrdU for >60 days to mice in remission and stopped it when the mice relapsed. 21 days later all CD11c^{hi} cells were BrdU$^{−}$ (data not shown) indicating they had been replaced, whereas 34.1 +/−11.7% of F4/80^{hi} cells were still BrdU^{+} (Figure 2G) indicating they had been present at the time of relapse. Both BrdU^{+} and BrdU$^{−}$ populations had upregulated CD11b (MFI in relapsed mice 72900 +/− 8661; p = NS compared with nephritic controls - compare Figure 2G with 2C and 2F). In sum these data suggest that activation of F4/80^{hi} cells, as assessed by upregulation of CD11b, occurs in situ and this activation reverses upon remission induction. In contrast the renal CD11c^{hi} population turns over rapidly and rapidly clears from the kidneys upon remission induction.

Origins of renal F4/80^{hi} macrophages

We used latex beads to label PBMCs in nephritic NZB/W mice. Beads were endocytosed into peripheral Gr1^{lo} cells (Figure 3A, B) and three days later were detected only within the renal F4/80^{hi} population (Figure 3C, D, H). No beads were detected in renal lymph nodes (Figure 3E) or thymus (Figure 3F), although a small number was detected in the spleen (Figure 3G). Thus, peripheral blood Gr1^{lo} monocytes are the precursors of the renal F4/80^{hi} population. CD11b expression was higher on renal cells than on matched peripheral blood cells (data not shown) consistent with our conclusion that activation of this cell population occurs in situ in the kidneys.

The 3 major renal mononuclear phagocyte populations have different morphologies

Cells were sorted into subpopulations shown in Figure 4A. Isolated F4/80^{lo} cells were round, with large nuclei and little cytoplasm, consistent with a macrophage phenotype (Figure 4B). In young and remission mice F4/80^{hi} cells were large and round with kidney shaped nuclei and small dendrites (Figure 4C). In nephritic mice the F4/80^{hi} cells became swollen and contained multiple double membrane vacuoles characteristic of autophagocytic vacuoles (Figure 4D, 4G–H). Oil RedO stain was negative for lipid (data not shown). CD11c^{hi} cells were large with many dendrites (Figure 4E) and had a veiled morphology by electron microscopy consistent with a myeloid DC phenotype (Figure 4E).

Renal mononuclear phagocyte subsets have different functional properties

The F4/80^{hi} population in nephritic mice had a significant increase in both cathepsin and MMP activity; no increase in either cathepsin or MMP activity was detected in the F4/80^{lo} population and there was only a modest increase in cathepsin activity in CD11c^{hi} cells (Figure 5A–D). Phagocytic activity was a property of the F4/80^{hi} population (3.3 +/− 1.3% of the F4/80^{hi} population vs. 1.3 +/− 0.3% of the CD11c^{hi} population after 30 minutes $p<0.05$ - Figure 5E) and did not change significantly in nephritic mice (not shown).

Affymetrix microarrays were performed using cDNA from sorted NZB/W F4/80^{hi} cells. We found 694 genes differentially expressed in nephritic kidneys compared with young kidneys (q-value < 0.01, fold-change ≥ 1.5 and ≤ 0.7 for the up-regulated and down-regulated genes respectively) (Supplementary Table I) and 794 genes differentially expressed in remission compared with nephritic kidneys (Supplementary Table II). 378 genes overlapped between the two comparisons and thus were biomarkers of nephritis activity (Supplementary Table III). Only 12 genes were differentially regulated between young and remission kidneys. We examined the 378 co-regulated genes in more detail using the natural language processing

tool (Genomatix BiblioSphere™) (26, 27). Transcriptional network analysis integrating these 378 differentially regulated mRNAs with literature mining (PubMed database) and automated promoter analysis, highlighted ITGAM, Stat3, TIMP-1, IL-10 and CCL-2 among important regulatory nodes (Figure 6 and Supplementary Table IV).

We chose a panel of 75 genes with varying degrees of upregulation at nephritis onset, and a set of control genes for confirmatory studies using quantitative RT-PCR. 6 additional genes specific for M1/M2 macrophage genotype but without significant differences by microarray, were also included. Using cut-off values of two fold overexpression and a q-value < 0.05, 49/75 genes were significantly different between young and nephritic mice and 50/75 were significantly different between nephritic mice and treated mice. There was 94% overlap between these two gene sets (Figure 7 and Supplementary Table V).

Pathway analysis using GePS (Genomatix Pathway System) (28) was performed on the 694 and 794 gene lists. The top 10 canonical pathways and signal transduction pathways (Genomatix literature mining) are displayed in Table I. Prothrombotic and tissue degradation pathways were among the most significantly regulated canonical pathways in nephritic compared to young kidney macrophages and interleukin 10 was the top significant signal transduction pathway. 28 genes of this pathway were altered in the macrophages from remission compared to nephritic kidneys. The top functions identified using Ingenuity Pathway Analysis software (IPA) included inflammatory response, cell-to-cell signaling and interaction, hematological system development and function, and immune cell trafficking

The gene expression studies revealed a mixed phenotype with expression of pro-inflammatory and anti-inflammatory genes as well as genes involved in tissue repair. We have confirmed increased protein expression of CD11b, and MMP14 previously (20, 29). To confirm increased protein expression of CXCL13, IL-10 and IKKε we performed immunohistochemistry, flow cytometry and Western blotting (Figure 8). To determine whether the presence of cathepsin activity could distinguish populations of F4/80^{hi} cells with different gene expression profiles we sorted Prosense^{hi} and ^{lo} subsets from nephritic mice and Prosense^{lo} cells from young mice and performed real-time PCR for expression of IL-10 (regulatory), IKKε, Mincle (inflammatory), TIMP-1, and MMP14 (repair). Cells from young mice had low expression of all markers whereas increased expression of all markers was observed in both Prosense hi and lo populations from nephritic mice with no difference in expression between the two populations (Figure 5F). In accord with these data, we were unable to distinguish F4/80^{hi} subpopulations on the basis of intracellular IKKε staining (Figure 8B).

DISCUSSION

Renal mononuclear phagocyte infiltration is associated with poor disease outcome in SLE nephritis (1). In this study of NZB/W lupus prone mice we show that there is an expansion of two major populations of mononuclear phagocytes nephritic kidneys. The renal F4/80^{hi} population is the major population in normal and pre-nephritic kidneys and has a CD11b^{hi}/CD11c^{int}/F4/80^{hi}/Gr1^{lo}/Ly6C^{lo}/VLA4^{lo}/MHCII^{hi}/CD80^{hi}/CD43^{lo}/CD62L^{lo} phenotype. This population is derived from circulating Gr1^{lo} monocytes that migrate into nephritic kidneys where they become activated in situ and form a cuff around glomeruli and around the edge of large interstitial inflammatory infiltrates (20). Nephritic NZB/W kidneys additionally accumulate a population of CD11b^{hi}/CD11c^{hi}/F4/80^{int}/MHCII^{lo}/Gr1^{lo}/VLA4^{hi}/CD43^{hi}/CD62L^{lo} myeloid dendritic cells that are located only within lymphoid aggregates (20) and disappear upon remission induction. Differences in the location of dendritic cells and macrophages has similarly been observed in human SLE kidney biopsies (14). Notably, the CD11b^{hi}/Ly6C^{hi}/VLA4^{hi}/CD43^{lo}/CD62L^{hi} inflammatory macrophage population (17) that

is found in most models of acute renal inflammation remains a minor population in NZB/W mice and in two other murine SLE models we have studied (30, 31).

The two major renal mononuclear phagocyte populations are functionally distinct. The F4/80^{hi} population is phagocytic and acquires both MMP and cathepsin activity at nephritis onset. The cells also increase their volume due to the accumulation of autophagocytic vacuoles. Intracellular degradation of cytoplasmic proteins and organelles by autophagy is required for Type I IFN responses to viral infections (32) but is also a physiologic response to inflammation or cellular stress and can be induced in human macrophages in vitro by exposure to growth factors and IL-10 (33). Although this process conserves energy, protects the cell from death and helps clear apoptotic bodies (34), it may enhance presentation of nuclear and cytosolic antigens (35, 36) and facilitate inflammation (37). In contrast, the CD11c^{hi} population is weakly phagocytic, downregulates expression of MHC Class II, and does not acquire MMP activity or accumulate autophagocytic vesicles. Downregulation of MHC Class II has been observed in dendritic cells exposed to hypoxia (38) or activated by cytokines including IL-10 (39).

To further understand why infiltrating F4/80^{hi} cells are associated with tissue damage we performed gene expression analysis on isolated cell populations from young, nephritic and remission mice. One goal of our gene expression analysis was to gain insight into mechanisms by which renal F4/80^{hi} macrophages contribute to pathogenesis of lupus nephritis by determining whether they exhibit features of classical or alternative activation. In addition to immune complexes and TLR ligands that promote an M2b phenotype, lupus nephritic macrophages are exposed to opposing signals from TNFα and tissue damage, and we hypothesized they may exhibit a mixed or potentially novel phenotype. Our data demonstrates that extensive changes in gene expression occur at proteinuria onset and reverse with remission induction. Surprisingly, we found that the expression profile has features consistent with a regulatory phenotype (7, 40) including expression of IL-10, PPARγ, anti-apoptotic genes, cytokine inhibitors such as IL1-RA and IL-18 binding protein, efferocytosis receptors such as Mer kinase and transglutaminase 2 and anti-inflammatory receptors such as the Prostaglandin E2 receptor. Induction of SOCS3 is associated with failure to upregulate IL-6 and TNFα. There is an increase in CD11b, an integrin required for cell activation, adhesion and phagocytosis, but whose engagement can also mediate negative feedback on TLR pathways and induce the production of IL-10 (11, 41).

The expression profile also displays a pro-inflammatory phenotype. Pro-inflammatory genes include Trem-1, an ITAM containing cell surface molecule that amplifies TLR mediated responses (42), activating Fc receptors and formyl peptidyl receptors, C-type lectins associated with tissue injury such as Mincle (43) and oxidized LDL receptor 1 (44, 45), chemokines such as CCL2, CCL5, CCL7 and CCL8 and costimulatory molecules such as CD80 and CD40. We also detected increased expression of C3, complement factor B and properdin suggesting a role of the activated F4/80^{hi} population in amplification of the alternative complement pathway (46); this, together with increased production of coagulation factors could propagate endothelial damage and thrombosis. The cells also upregulate CXCL13, a chemokine that can be induced by IL-10 as well as by IL-1 and TNFα (11, 47, 48) and that helps to orchestrate lymphoid neogenesis in inflamed tissues. Finally, we observed expression of MMPs and cathepsin proteases that are associated with tissue repair during the resolution of acute inflammation, but could mediate tissue degradation if chronically expressed.

Many of the pro-inflammatory genes expressed by activated renal macrophages in nephritic NZB/W kidneys are induced in human macrophages by TNFα (L Ivashkiv, unpublished data), but not by the ITAM cross-linking that induces a regulatory macrophage phenotype.

TNFα, made by multiple cell types in inflamed kidneys including non-lymphoid renal cells (20), is pathogenic in the effector phase of SLE nephritis (49). One gene induced by TNFα and highly upregulated in F4/80^{hi} cells from nephritic kidneys is IKKε (IKKi), a kinase that enhances the induction of a subset of NFκB regulated genes and phosphorylates the transcription factors IRF-3 and IRF-7, major inducers of Type I interferons. IKKε phosphorylates STAT1 and enhances formation of the ISGF3 transcriptional complex (50) that helps mediate some of the inhibitory and anti-proliferative effects of Type I IFNs (51, 52). IKKε is dispensable for acute inflammatory responses (53). In contrast, its expression is markedly upregulated in F4/80^{hi} macrophages derived from chronically inflamed adipose tissue of mice fed a high fat diet and it is essential for maintaining low grade inflammation and propagating obesity in these mice (53). IKKε deficient mice are less sensitive to arthritis induction in a passive transfer model; inhibition of Type I IFNs and IKKε is therapeutic in this disease (54). These observations suggest a role for IKKε in chronic inflammation.

We have confirmed increased protein expression of CD11b, CD80, CD86, MMP2, MMP14, Ikkε, CXCL13 and IL-10 and the presence of functional cathepsin and MMP activity in the F4/80^{hi} macrophage population of nephritic mice in this and previous studies [Figures 5 & 8 and (20, 29)]. Further work will be needed to confirm protein expression of other genes in the expression profile and to determine whether the macrophages express the genes comprising the hybrid profile simultaneously, whether there are different subsets expressing different aspects of the profile or whether the mixed phenotype reflects an evolution of one type of macrophage from another.

Our data, in sum, point to a unique activation profile of macrophages and dendritic cells in SLE kidneys quite different to that found in acute renal inflammation or ischemia. We surmise that this phenotype results from chronic exposure of SLE kidney macrophages to immune complexes, cytokines such as TNFα, TLR signals, fibrinogen, dead and dying cells, hypoxia and other danger signals. The resultant mixed phenotype is associated with chronic and progressive renal injury. The M1-like characteristics of kidney macrophages likely contribute to the local inflammatory process but it is less clear if the M2 components of the phenotype are protective or pathogenic. It is possible that expression of M2 genes that are utilized to resolve inflammation or repair tissues in other settings ‘inadvertently’ contributes to pathogenesis by promoting excessive tissue remodeling and linked proliferation.

Another striking finding is that pathway analysis identified central roles for genes with allelic polymorphisms that have been linked to SLE including *Il10, Itgam, Ptpn22, Atg5 and IRF7*. The pathogenic role of IL-10 secreting macrophages in chronic inflammation has been suggested by our previous studies in NZB/W mice with proliferative glomerulonephritis accelerated by Type I IFNs. In these studies, depletion of IL-10 producing phagocytic renal macrophages prevented ongoing crescent formation and renal damage (29). IL-10 may also augment mesangial proliferation in inflamed kidneys (29, 55). IL-10 antagonism is therapeutic in NZB/W mice (56) and a small clinical study of anti-IL-10 in humans showed salutary effects (57). It will be worthwhile in future studies to examine the function of the other molecules identified in genetic studies specifically in macrophages and dendritic cells.

There has been much recent interest in manipulating macrophage programming and migration in acute renal diseases. Therapeutic targeting of key molecules identified here in the murine models should help to define the function of the major renal mononuclear phagocyte cell types found in SLE kidneys. An enhanced understanding of macrophage and DC phenotypes and function in patients with SLE nephritis will be needed in order to appropriately target these cell populations in humans.

Supplementary Material

Refer to Web version on PubMed Central for supplementary material.

Acknowledgments

The authors thank Haiou Tao for technical assistance and Stella Stefanova for assistance with cell sorting. The authors thank Drs Yong Du and Chandra Mohan for the gift of kidneys from anti-GBM mice.

References

1. Hill GS, Delahousse M, Nochy D, Remy P, Mignon F, Mery JP, Bariety J. Predictive power of the second renal biopsy in lupus nephritis: significance of macrophages. Kidney Int. 2001; 59:304–316. [PubMed: 11135084]
2. Sean Eardley K, Cockwell P. Macrophages and progressive tubulointerstitial disease. Kidney Int. 2005; 68:437–455. [PubMed: 16014021]
3. Knight SF, Quigley JE, Yuan J, Roy SS, Elmarakby A, Imig JD. Endothelial dysfunction and the development of renal injury in spontaneously hypertensive rats fed a high-fat diet. Hypertension. 2008; 51:352–359. [PubMed: 18158349]
4. Bergtold A, Gavhane A, D'Agati V, Madaio M, Clynes R. FcR-bearing myeloid cells are responsible for triggering murine lupus nephritis. J Immunol. 2006; 177:7287–7295. [PubMed: 17082647]
5. Mosser DM. The many faces of macrophage activation. J Leukoc Biol. 2003; 73:209–212. [PubMed: 12554797]
6. Mantovani A, Sica A, Sozzani S, Allavena P, Vecchi A, Locati M. The chemokine system in diverse forms of macrophage activation and polarization. Trends Immunol. 2004; 25:677–686. [PubMed: 15530839]
7. Mosser DM, Edwards JP. Exploring the full spectrum of macrophage activation. Nat Rev Immunol. 2008; 8:958–969. [PubMed: 19029990]
8. Hume DA. Differentiation and heterogeneity in the mononuclear phagocyte system. Mucosal Immunol. 2008; 1:432–441. [PubMed: 19079210]
9. Gordon S, Martinez FO. Alternative activation of macrophages: mechanism and functions. Immunity. 2010; 32:593–604. [PubMed: 20510870]
10. Martinez FO, Sica A, Mantovani A, Locati M. Macrophage activation and polarization. Front Biosci. 2008; 13:453–461. [PubMed: 17981560]
11. Wang L, Gordon RA, Huynh L, Su X, Park Min KH, Han J, Arthur JS, Kalliolias GD, Ivashkiv LB. Indirect inhibition of Toll-like receptor and type I interferon responses by ITAM-coupled receptors and integrins. Immunity. 2010; 32:518–530. [PubMed: 20362473]
12. Kruger T, Benke D, Eitner F, Lang A, Wirtz M, Hamilton-Williams EE, Engel D, Giese B, Muller-Newen G, Floege J, Kurts C. Identification and functional characterization of dendritic cells in the healthy murine kidney and in experimental glomerulonephritis. J Am Soc Nephrol. 2004; 15:613–621. [PubMed: 14978163]
13. Soos TJ, Sims TN, Barisoni L, Lin K, Littman DR, Dustin ML, Nelson PJ. CX3CR1+ interstitial dendritic cells form a contiguous network throughout the entire kidney. Kidney Int. 2006; 70:591–596. [PubMed: 16760907]
14. Segerer S, Heller F, Lindenmeyer MT, Schmid H, Cohen CD, Draganovici D, Mandelbaum J, Nelson PJ, Grone HJ, Grone EF, Figel AM, Nossner E, Schlondorff D. Compartment specific expression of dendritic cell markers in human glomerulonephritis. Kidney Int. 2008; 74:37–46. [PubMed: 18368027]
15. Ferenbach D, Hughes J. Macrophages and dendritic cells: what is the difference? Kidney Int. 2008; 74:5–7. [PubMed: 18560360]
16. Geissmann F, Auffray C, Palframan R, Wirrig C, Ciocca A, Campisi L, Narni-Mancinelli E, Lauvau G. Blood monocytes: distinct subsets, how they relate to dendritic cells, and their possible

roles in the regulation of T-cell responses. Immunol Cell Biol. 2008; 86:398–408. [PubMed: 18392044]

17. Li L, Huang L, Sung SS, Vergis AL, Rosin DL, Rose CE Jr, Lobo PI, Okusa MD. The chemokine receptors CCR2 and CX3CR1 mediate monocyte/macrophage trafficking in kidney ischemia-reperfusion injury. Kidney Int. 2008; 74:1526–1537. [PubMed: 18843253]
18. Kurts C. Dendritic cells: not just another cell type in the kidney, but a complex immune sentinel network. Kidney Int. 2006; 70:412–414. [PubMed: 16871253]
19. Schiffer L, Sinha J, Wang X, Huang W, von Gersdorff G, Schiffer M, Madaio MP, Davidson A. Short term administration of costimulatory blockade and cyclophosphamide induces remission of systemic lupus erythematosus nephritis in NZB/W F1 mice by a mechanism downstream of renal immune complex deposition. J Immunol. 2003; 171:489–497. [PubMed: 12817034]
20. Schiffer L, Bethunaickan R, Ramanujam M, Huang W, Schiffer M, Tao H, Madaio MP, Bottinger EP, Davidson A. Activated renal macrophages are markers of disease onset and disease remission in lupus nephritis. J Immunol. 2008; 180:1938–1947. [PubMed: 18209092]
21. Xie C, Sharma R, Wang H, Zhou XJ, Mohan C. Strain distribution pattern of susceptibility to immune-mediated nephritis. J Immunol. 2004; 172:5047–5055. [PubMed: 15067087]
22. Ramanujam M, Wang X, Huang W, Liu Z, Schiffer L, Tao H, Frank D, Rice J, Diamond B, Yu KO, Porcelli S, Davidson A. Similarities and differences between selective and nonselective BAFF blockade in murine SLE. J Clin Invest. 2006; 116:724–734. [PubMed: 16485042]
23. Nahrendorf M, Swirski FK, Aikawa E, Stangenberg L, Wurdinger T, Figueiredo JL, Libby P, Weissleder R, Pittet MJ. The healing myocardium sequentially mobilizes two monocyte subsets with divergent and complementary functions. J Exp Med. 2007; 204:3037–3047. [PubMed: 18025128]
24. Tusher VG, Tibshirani R, Chu G. Significance analysis of microarrays applied to the ionizing radiation response. Proc Natl Acad Sci U S A. 2001; 98:5116–5121. [PubMed: 11309499]
25. Ginhoux F, Liu K, Helft J, Bogunovic M, Greter M, Hashimoto D, Price J, Yin N, Bromberg J, Lira SA, Stanley ER, Nussenzweig M, Merad M. The origin and development of nonlymphoid tissue CD103+ DCs. J Exp Med. 2009; 206:3115–3130. [PubMed: 20008528]
26. Wiggins JE, Patel SR, Shedden KA, Goyal M, Wharram BL, Martini S, Kretzler M, Wiggins RC. NFkappaB promotes inflammation, coagulation, and fibrosis in the aging glomerulus. J Am Soc Nephrol. 2010; 21:587–597. [PubMed: 20150534]
27. Schmid H, Boucherot A, Yasuda Y, Henger A, Brunner B, Eichinger F, Nitsche A, Kiss E, Bleich M, Grone HJ, Nelson PJ, Schlondorff D, Cohen CD, Kretzler M. Modular activation of nuclear factor-kappaB transcriptional programs in human diabetic nephropathy. Diabetes. 2006; 55:2993–3003. [PubMed: 17065335]
28. Frisch M, Klocke B, Haltmeier M, Frech K. LitInspector: literature and signal transduction pathway mining in PubMed abstracts. Nucleic Acids Res. 2009; 37:W135–140. [PubMed: 19417065]
29. Triantafyllopoulou A, Franzke CW, Seshan SV, Perino G, Kalliolias GD, Ramanujam M, van Rooijen N, Davidson A, Ivashkiv LB. Proliferative lesions and metalloproteinase activity in murine lupus nephritis mediated by type I interferons and macrophages. Proc Natl Acad Sci U S A. 2010; 107:3012–3017. [PubMed: 20133703]
30. Ramanujam M, Kahn P, Huang W, Tao H, Madaio MP, Factor SM, Davidson A. Interferon-alpha treatment of female (NZW × BXSB)F(1) mice mimics some but not all features associated with the Yaa mutation. Arthritis Rheum. 2009; 60:1096–1101. [PubMed: 19333924]
31. Ramanujam M, Bethunaickan R, Huang W, Tao H, Madaio MP, Davidson A. Selective blockade of BAFF for the prevention and treatment of systemic lupus erythematosus nephritis in NZM2410 mice. Arthritis Rheum. 2010; 62:1457–1468. [PubMed: 20131293]
32. Orvedahl A, Levine B. Autophagy in Mammalian antiviral immunity. Curr Top Microbiol Immunol. 2009; 335:267–285. [PubMed: 19802570]
33. Santiago-Schwarz F, Valentino A, Martin C, DiMaio C. IL-10 interruption of dendritic cell (DC) differentiation during the monocyte-to-DC transition is associated with increased levels of LC3, mature autophagosome formation, and survival of monocyte-macrophage-like cells. Journal of Immunology. 2010; 184:134.121.

34. Qu X, Zou Z, Sun Q, Luby-Phelps K, Cheng P, Hogan RN, Gilpin C, Levine B. Autophagy gene-dependent clearance of apoptotic cells during embryonic development. Cell. 2007; 128:931–946. [PubMed: 17350577]
35. Crotzer VL, Blum JS. Autophagy and its role in MHC-mediated antigen presentation. J Immunol. 2009; 182:3335–3341. [PubMed: 19265109]
36. Munz C. Selective macroautophagy for immunity. Immunity. 2010; 32:298–299. [PubMed: 20346769]
37. Chang YP, Tsai CC, Huang WC, Wang CY, Chen CL, Lin YS, Kai JI, Hsieh CY, Cheng YL, Choi PC, Chen SH, Chang SP, Liu HS, Lin CF. Autophagy facilitates IFN-{gamma}-induced Jak2-STAT1 activation and cellular inflammation. J Biol Chem. 2010
38. Mancino A, Schioppa T, Larghi P, Pasqualini F, Nebuloni M, Chen IH, Sozzani S, Austyn JM, Mantovani A, Sica A. Divergent effects of hypoxia on dendritic cell functions. Blood. 2008; 112:3723–3734. [PubMed: 18694997]
39. Choi YE, Yu HN, Yoon CH, Bae YS. Tumor-mediated down-regulation of MHC class II in DC development is attributable to the epigenetic control of the CIITA type I promoter. Eur J Immunol. 2009; 39:858–868. [PubMed: 19224634]
40. Tabas I. Macrophage death and defective inflammation resolution in atherosclerosis. Nat Rev Immunol. 2010; 10:36–46. [PubMed: 19960040]
41. Han C, Jin J, Xu S, Liu H, Li N, Cao X. Integrin CD11b negatively regulates TLR-triggered inflammatory responses by activating Syk and promoting degradation of MyD88 and TRIF via Cbl-b. Nat Immunol. 2010; 11:734–742. [PubMed: 20639876]
42. Bouchon A, Facchetti F, Weigand MA, Colonna M. TREM-1 amplifies inflammation and is a crucial mediator of septic shock. Nature. 2001; 410:1103–1107. [PubMed: 11323674]
43. Yamasaki S, Ishikawa E, Sakuma M, Hara H, Ogata K, Saito T. Mincle is an ITAM-coupled activating receptor that senses damaged cells. Nat Immunol. 2008; 9:1179–1188. [PubMed: 18776906]
44. Pyz E, Marshall AS, Gordon S, Brown GD. C-type lectin-like receptors on myeloid cells. Ann Med. 2006; 38:242–251. [PubMed: 16754255]
45. Hu C, Kang BY, Megyesi J, Kaushal GP, Safirstein RL, Mehta JL. Deletion of LOX-1 attenuates renal injury following angiotensin II infusion. Kidney Int. 2009; 76:521–527. [PubMed: 19553911]
46. Holers VM. The spectrum of complement alternative pathway-mediated diseases. Immunol Rev. 2008; 223:300–316. [PubMed: 18613844]
47. Ishikawa S, Nagai S, Sato T, Akadegawa K, Yoneyama H, Zhang YY, Onai N, Matsushima K. Increased circulating CD11b+CD11c+ dendritic cells (DC) in aged BWF1 mice which can be matured by TNF-alpha into BLC/CXCL13-producing DC. Eur J Immunol. 2002; 32:1881–1887. [PubMed: 12115607]
48. Perrier P, Martinez FO, Locati M, Bianchi G, Nebuloni M, Vago G, Bazzoni F, Sozzani S, Allavena P, Mantovani A. Distinct transcriptional programs activated by interleukin-10 with or without lipopolysaccharide in dendritic cells: induction of the B cell-activating chemokine, CXC chemokine ligand 13. J Immunol. 2004; 172:7031–7042. [PubMed: 15153525]
49. Aringer M, Steiner G, Graninger WB, Hofler E, Steiner CW, Smolen JS. Effects of short-term infliximab therapy on autoantibodies in systemic lupus erythematosus. Arthritis Rheum. 2007; 56:274–279. [PubMed: 17195231]
50. Tenoever BR, Ng SL, Chua MA, McWhirter SM, Garcia-Sastre A, Maniatis T. Multiple functions of the IKK-related kinase IKKepsilon in interferon-mediated antiviral immunity. Science. 2007; 315:1274–1278. [PubMed: 17332413]
51. Laver T, Nozell SE, Benveniste EN. IFN-beta-mediated inhibition of IL-8 expression requires the ISGF3 components Stat1, Stat2, and IRF-9. J Interferon Cytokine Res. 2008; 28:13–23. [PubMed: 18370868]
52. Tsuno T, Mejido J, Zhao T, Schmeisser H, Morrow A, Zoon KC. IRF9 is a key factor for eliciting the antiproliferative activity of IFN-alpha. J Immunother. 2009; 32:803–816. [PubMed: 19752753]

53. Chiang SH, Bazuine M, Lumeng CN, Geletka LM, Mowers J, White NM, Ma JT, Zhou J, Qi N, Westcott D, Delproposto JB, Blackwell TS, Yull FE, Saltiel AR. The protein kinase IKKepsilon regulates energy balance in obese mice. Cell. 2009; 138:961–975. [PubMed: 19737522]

54. Corr M, Boyle DL, Ronacher L, Flores N, Firestein GS. Synergistic benefit in inflammatory arthritis by targeting I kappaB kinase epsilon and interferon beta. Ann Rheum Dis. 2009; 68:257–263. [PubMed: 18653628]

55. Kalechman Y, Gafter U, Weinstein T, Chagnac A, Freidkin I, Tobar A, Albeck M, Sredni B. Inhibition of interleukin-10 by the immunomodulator AS101 reduces mesangial cell proliferation in experimental mesangioproliferative glomerulonephritis: association with dephosphorylation of STAT3. J Biol Chem. 2004; 279:24724–24732. [PubMed: 15001575]

56. Ishida H, Muchamuel T, Sakaguchi S, Andrade S, Menon S, Howard M. Continuous administration of anti-interleukin 10 antibodies delays onset of autoimmunity in NZB/W F1 mice. J Exp Med. 1994; 179:305–310. [PubMed: 8270873]

57. Lauwerys BR, Garot N, Renauld JC, Houssiau FA. Interleukin-10 blockade corrects impaired in vitro cellular immune responses of systemic lupus erythematosus patients. Arthritis Rheum. 2000; 43:1976–1981. [PubMed: 11014347]

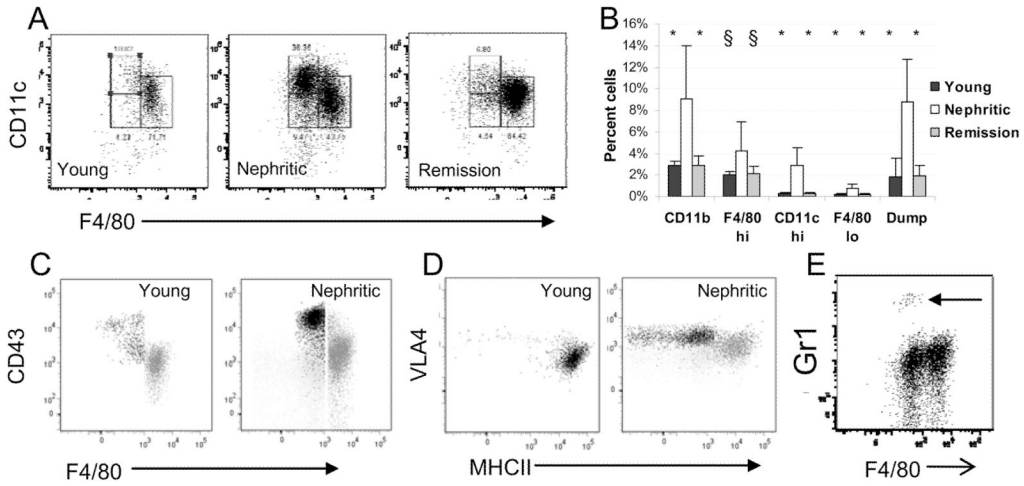

Figure 1.

Flow cytometric analysis of renal mononuclear phagocytes: Gating strategy for CD11b^{hi} cells is shown in Figure S1. A: Gating strategy for the F4/80^{hi} (right), F4/80^{lo} (lower left) and CD11c^{hi} (upper left) subpopulations of CD11b^{hi} cells. B: The increase in the percentage of CD11b^{hi} cells as a percent of live cells in the kidneys of nephritic mice is accounted for mainly by an increase in the F4/80^{hi} population and an influx of CD11c^{hi} cells. There is an increase in lymphocyte infiltration (percent cells in the dump gate) in nephritic mice. Cellular infiltration resolves upon remission induction. (Young and remission mice compared with nephritic mice – 6–8 mice per group; * $p < 0.002$; § $p < 0.05$,). C: CD43 staining of the CD11c^{hi} (black) and F4/80^{hi} (grey) populations from young and nephritic mice. Light grey is isotype control for CD43. D: VLA4 and MHCII staining of the CD11c^{hi} (black) and F4/80^{hi} (grey) populations from young and nephritic mice. Light grey is isotype control for VLA4. E: Gr1 staining shows a small population of neutrophils in nephritic mice (arrow). Plots are representative of at least 5 mice per group. Experiments were repeated > 3 times.

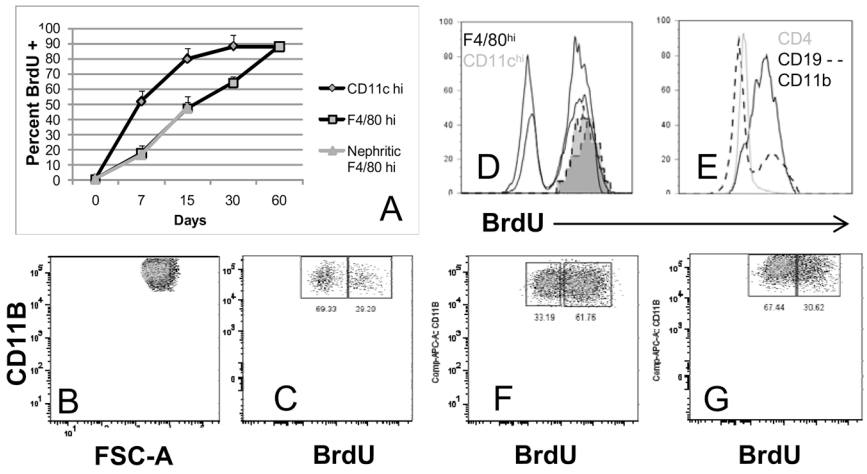

Figure 2.

Analysis of renal mononuclear phagocyte turnover: Mice were fed BrdU from Days 2–40 after remission induction (B–F) or for > 60 days after remission induction followed by BrdU withdrawal at relapse (G). B, C, F and G represent cells gated on CD11b and F4/80^{hi}. A. BrdU uptake over time in NZB/W mice (4 mice per group). B–C: Downregulation of CD11b expression 21 days after remission (C) compared with nephritic control (B) occurs in both the BrdU+ (newly arrived) and BrdU− (resident) population of F4/80^{hi} cells. D: 21 days after remission all Cd11c^{hi} cells (2 shaded histograms) are BrdU+, whereas many F4/80^{hi} cells (2 black histograms) are still BrdU−. E: 21 days after remission CD11b+ cells in the spleens are nearly all BrdU+, compared with only a small proportion of B cells and T cells. F: 40 days after remission induction 1/3 of F4/80^{hi} cells are still BrdU−. G: 21 days after relapse, upregulation of CD11b is evident in both the BrdU+ (resident) and BrdU− (newly arrived) population of F4/80^{hi} cells. Data for B–G are representative of 4 mice per group. Experiments were repeated once.

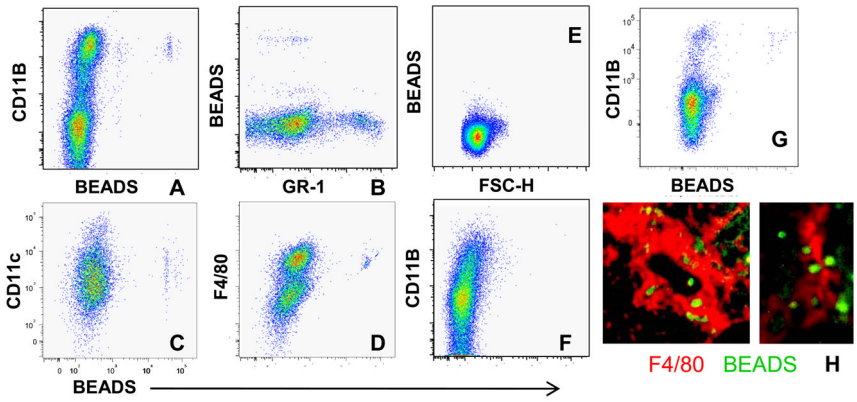

Figure 3.

In vivo labeling of PBMCs 3 days after administration of Latex beads: A–B: Uptake of fluorescent beads occurs in the peripheral blood $CD11b^{hi}/F4/80^{lo}/Gr1^{lo}$ population. C–D: Bead laden cells are restricted to the $F4/80^{hi}$ population of renal $CD11b^{hi}$ cells. E-G: No beads are detected in the renal node (E) or thymus (F) but there is some trafficking to $CD11b^{+}$ cells in the spleen (G). H: Immunofluorescence analysis of kidneys shows beads within $F4/80^{hi}$ cells (magnification 10x and 40x). Data are representative of 5 mice per group. Experiments were repeated once.

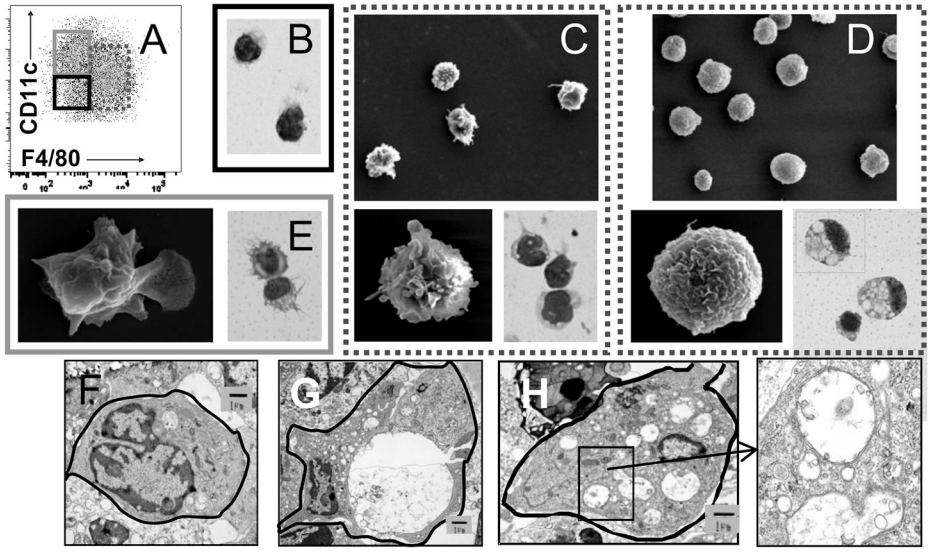

Figure 4.

Morphology of renal mononuclear phagocytes by Wright Giemsa staining and scanning electron microscopy: A: Gating strategy for sorting of F4/80^{hi} (dashed), CD11c^{hi} (grey) and F4/80^{lo} (black) populations (see also Figure S1). B: The F4/80^{lo} population consists of round macrophage like cells and some neutrophils (not shown). C–D: There is an increase in volume and marked vacuolization of the F4/80^{hi} population in nephritic mice (D) compared with that of young mice (C). E: the CD11c^{hi} population has a veiled morphology characteristic of dendritic cells. Magnification 100X for Wright Giemsa stains and 750X and 10,000X for electron microscopy. E–H: Representative transmission electron microscope visualization of F4/80^{hi} cells from young (F) and nephritic mice (G,H) show multiple vacuoles in the nephritic mice many of which have double membranes (inset from H). Data are representative of 3–4 mice per group. Experiments were repeated once.

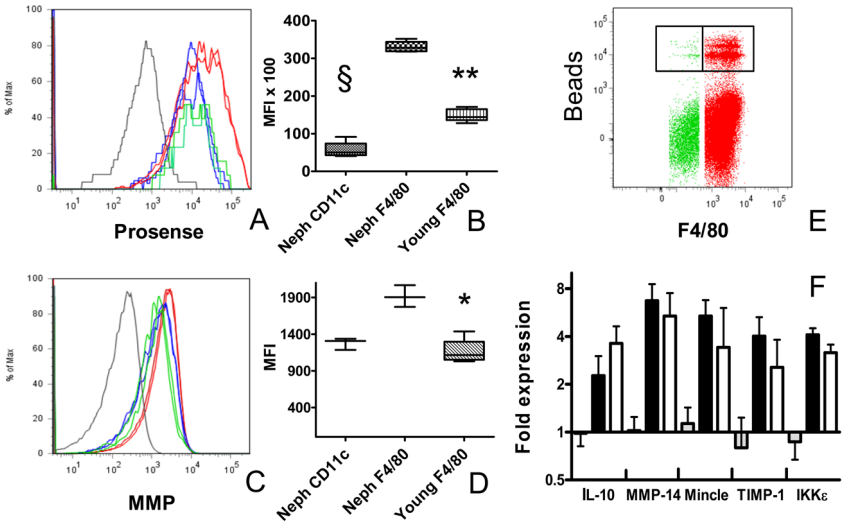

Figure 5.

Functional studies of renal mononuclear phagocytes: A: In vivo cathepsin labeling of young F4/80^{hi} cells (green), nephritic F4/80^{hi} cells (red) and nephritic CD11c^{hi} cells (blue). CD11b^{-} lymphocytes are shown in grey. B: MFI values for cathepsin activity (** $p<0.02$ § $p < 0.01$). C: In vivo MMP activity of young F4/80^{hi} cells (green), nephritic F4/80^{hi} cells (red) and nephritic CD11c^{hi} cells (blue). CD11b− lymphocytes are shown in grey. D: MFI values for MMP labeling (* $p < 0.05$). E: In vitro phagocytosis assay shows that the majority of bead uptake is in the renal F4/80^{hi} population (green) compared with the CD11c^{hi} population (red). Beads were incubated with renal cells for 45 minutes in this experiment. F: RNA from Sorted F4/80^{hi} Prosense^{hi} (grey; young; black: nephritic) and Prosense^{lo} (white: nephritic) cells was analyzed by real-time PCR. Data are representative of at least 4 mice per group. Experiments were repeated twice.

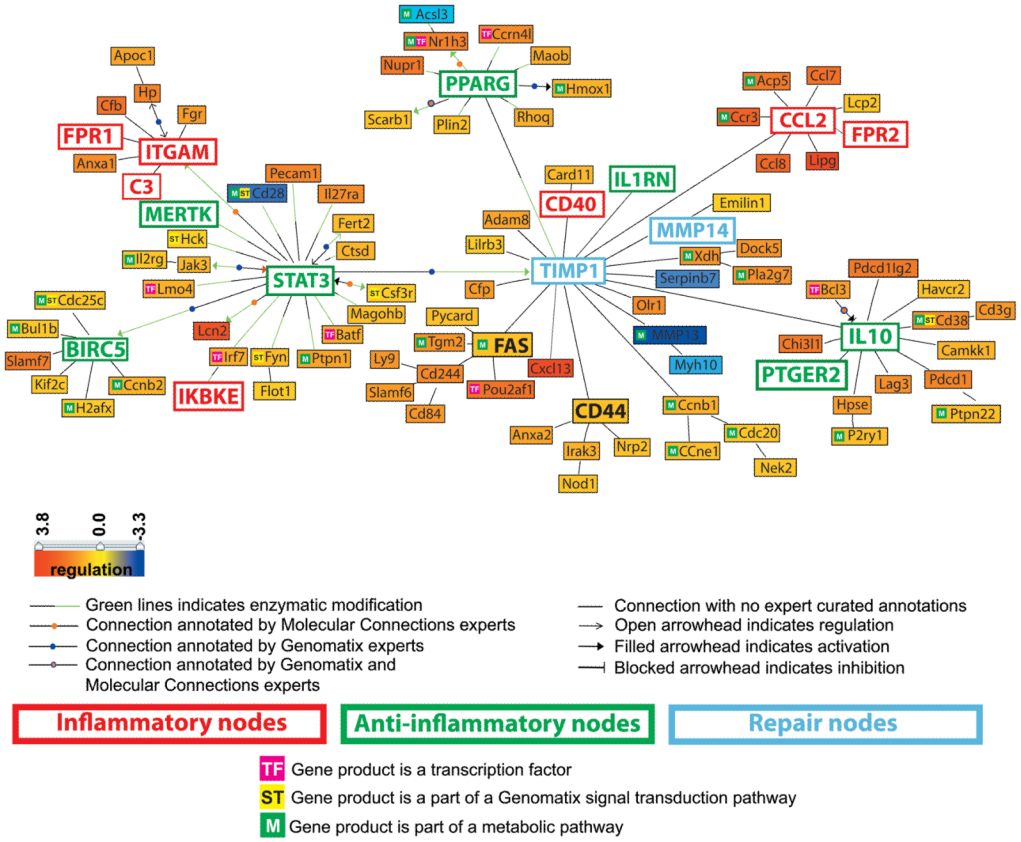

Figure 6.

Literature-based analysis using Genomatix - Bibliosphere software of the genes that were regulated in F4/80^{hi} cells from nephritic kidneys (n = 7) compared to both young (n = 6) and remission (n = 4) kidneys (with stringent filter criteria: q-value <0.001, fold-change ≥ 1.5 and ≤ 0.7 for the up-regulated and down-regulated genes respectively). The picture shows the 101 genes that were co-cited in PubMed abstracts in the same sentence linked by a function word (B3 filter). Yellow to red represents the genes that are upregulated and yellow to blue represents the genes that are downregulated in nephritic compared to young mice.

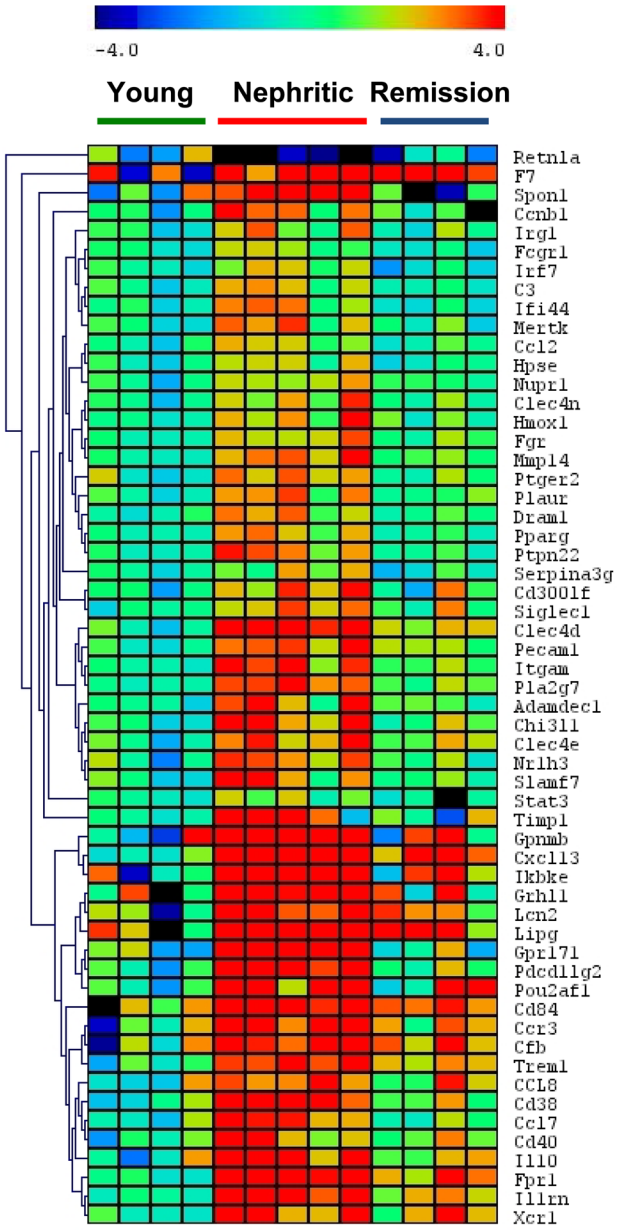

Figure 7.

One way cluster analysis of genes with significantly altered expression in the PCR confirmation set (See Supplementary Table V). Gene expression was normalized to the mean of 3 housekeeping genes as described in materials and methods. Significantly up or downregulated (> 2 fold) genes by SAM are shown.

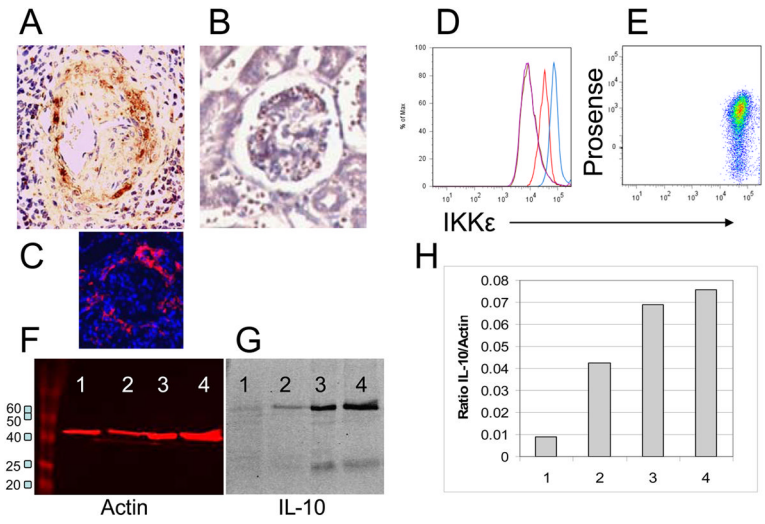

Figure 8.

Protein expression of analytes of interest. A: CXCL13 staining was observed in periglomerular infiltrates of nephritic mice (A) but not young controls (B). Periglomerular F4/80^{hi} macrophages were preset only in nephritic mice (C: same mouse as A). D: Intracellular IKKε staining was significantly increased in F4/80^{hi} cells of nephritic mice (blue) compared with young mice (red) and isotype controls (purple). E: IKKε staining was uniform in both Prosense hi and lo populations from nephritic mice. F-G: Western blot for IL-10 in sorted F4/80^{hi} renal cells from young NZB/W mice (Lane 1), mice with new onset proteinuria (Lane 2) and mice with established proteinuria (Lanes 3,4). Red bands show actin control and panel H shows IL-10/actin ratio.

Table I

Top 10 canonical and signal transduction pathways (Genomatix literature mining) as assessed by GePS (Genomatix Pathway System software).

From the 694 genes regulated in macrophages from nephritic vs. young kidneys				
Canonical pathways (number of genes in the pathway)		**p-value**	**No. regulated genes**	**No. expected genes**
1	Extrinsic prothrombin activation pathway (14)	2.57E-04	5	0.63
2	IL12-mediated signaling events (63)	1.83E-03	9	2.86
3	FOXM1 transcription factor network (42)	2.41E-03	7	1.90
4	Fibrinolysis pathway (16)	4.81E-03	4	0.73
5	Inhibition of matrix metalloproteinases (9)	6.27E-03	3	0.41
6	Aurora B signaling (41)	9.45E-03	6	1.86
7	Co-stimulatory signal during T-cell activation (20)	1.11E-02	4	0.91
8	Phospholipase c delta in phospholipid associated cell signaling (4)	1.15E-02	2	0.18
9	PLK1 signaling events (47)	1.81E-02	6	2.13
10	Basic mechanism of action of ppara pparb(d) and pparg and effects on gene expression (5)	1.86E-02	2	0.23
Signal transduction pathway (number of genes in the pathway)				
1	Interleukin 10 (265)	1.66E-09	40	14.27
2	NF kappa B (1341)	3.13E-09	118	72.24
3	Toll like receptor (398)	8.85E-09	50	21.44
4	Integrin (458)	2.00E-08	54	24.67
5	Interleukin 1 (623)	3.26E-08	66	33.56
6	Signal transduction and activator of transcription (1002)	4.90E-08	92	53.98
7	Interleukin 1 receptor (103)	8.80E-08	21	5.55
8	Interleukin 6 (Interferon, beta 2) (581)	1.68E-07	61	31.30
9	Tumor necrosis factor (TNF superfamily, member 2) (1035)	2.35E-07	92	55.75
10	Tumor necrosis factor receptor superfamily (826)	4.71E-07	77	44.49
From the 794 genes regulated in macrophages from remission vs. nephritic kidneys				
Canonical pathways (number of genes in the pathway)				
1	Aurora B signaling (41)	4.15E-10	16	2.46
2	PLK1 signaling events (47)	4.39E-09	16	2.82
3	FOXM1 transcription factor network (42)	4.76E-07	13	2.52
4	Cdk regulation of dna replication (18)	4.54E-05	7	1.08
5	Aurora A signaling (31)	5.32E-05	9	1.86
6	IL12-mediated signaling events (63)	6.36E-05	13	3.78
7	Alternative NF-kappaB pathway (6)	3.72E-03	3	0.36
8	IL12 signaling mediated by STAT4 (36)	4.73E-03	7	2.16
9	TCR signaling in naive CD8+ T cells (56)	5.40E-03	9	3.36
10	The co-stimulatory signal during t-cell activation (20)	5.46E-03	5	1.20
Signal transduction pathway (number of genes in the pathway)				

From the 694 genes regulated in macrophages from nephritic vs. young kidneys				
Canonical pathways (number of genes in the pathway)		**p-value**	**No. regulated genes**	**No. expected genes**
1	Aurora kinase (85)	3.67E-11	25	5.40
2	Cell division cycle 2 (G1 to S and G2 to M) (216)	1.18E-10	41	13.72
3	Signal transduction and activator of transcription (1002)	4.13E-10	111	63.66
4	Polo like kinase 1 (109)	2.33E-09	26	6.93
5	Integrin (458)	2.98E-08	60	29.10
6	Interleukin 12 (217)	2.18E-07	35	13.79
7	Janus kinase (560)	3.49E-07	66	35.58
8	Interleukin 1 (623)	4.36E-07	71	39.58
9	Interleukin 10 (265)	5.16E-07	39	16.84
10	Guanine nucleotide exchange factor VAV (211)	1.01E-06	33	13.41